

Self-Calibration of Cluster Dark Energy Studies: Counts in Cells

Marcos Lima¹ and Wayne Hu²

¹*Department of Physics,*

University of Chicago, Chicago IL 60637

²*Center for Cosmological Physics,*

Department of Astronomy and Astrophysics,

and Enrico Fermi Institute,

University of Chicago, Chicago IL 60637

Cluster number counts can constrain the properties of dark energy if and only if the evolution in the relationship between observable quantities and the cluster mass can be calibrated. Next generation surveys with $\sim 10^4$ clusters will have sufficient statistics to enable some degree of self-calibration. The excess variance of counts due to the clustering of clusters provides such an opportunity and can be measured from the survey without additional observational cost. It can minimize the degradation in dark energy constraints due to an unknown power law evolution in the mass-observable relation improving constraints on the dark energy equation of state by a factor of 2 or more to $\sigma(w) = 0.06$ for a deep 4000 deg² survey.

I. INTRODUCTION

The abundance of clusters of galaxies of a known mass is a sensitive probe of linear density fluctuations given Gaussian random initial conditions (e.g. [1]). Since the growth of fluctuations is halted by the dark energy, abundance measurements as a function of redshift can be translated into dark energy constraints [2, 3].

Unfortunately, the mass of a cluster is not a direct observable. The key to exploiting this dark energy sensitivity is to determine the relationships between observable quantities such as flux or temperature and the mass. *Ab initio* computations from cosmological simulations serve as useful guides but invite misinterpretation when used directly due to missing gas, star formation, and AGN physics (e.g. [4, 5]). Much like with the distance ladder determinations of the Hubble constant, more progress can be made by cross-calibrating the mass-observable relations between X-ray, lensing, optical and microwave surveys. A potential drawback is that cross-calibration makes the interpretation of each data set subject to the systematic errors in all of the surveys employed and so the weakest link in the chain. Cross-calibration can also only be performed across the redshift and mass range where surveys overlap.

Recently, self-calibration techniques have been advocated as a useful check on cross-calibration and the internal consistency of dark energy determinations. Clusters benefit from having several mass-sensitive properties that can be reliably predicted from simulations of their dark matter properties only. The first of course is the evolution of the abundance itself. An unknown constant normalization of the mass-observable relation can be determined from the evolution in the abundance above threshold in the given observable [6]. Even an arbitrarily evolving normalization can be determined by measuring the abundance as a function of the threshold and redshift [7]. This technique however requires a dy-

namic range in the mass function that is substantially larger than the scatter in the mass-observable relation and will only be possible with very deep surveys or at fairly low redshifts. Finally, mild evolution in the mass-observable relation can be calibrated by examining the power spectrum of the clusters [8]. The drawback of the latter method is that measuring the three dimensional power spectrum generally requires precise redshifts and hence costly spectroscopy or an improvement in photometric redshift techniques beyond that required for abundance studies themselves ($\Delta z \approx 0.1$).

Here we point out that there is an analog of the power spectrum self-calibration technique that will automatically come out of the statistical analysis of the number counts in any given cluster survey. The excess or sample variance of the counts due to the clustering of clusters must be included in future error analyses [9]. For self-calibration purposes, this source of “noise” is actually signal and can be used to calibrate the mass observable relation.

II. NOISE AS SIGNAL

The probability of measuring a number of clusters N in a cell of a given redshift z and angular extent is given by the Poisson distribution

$$P(N|m) = \frac{m^N}{N!} e^{-m}, \quad (1)$$

where the mean $m \equiv \langle N \rangle_P$ and the brackets denote averaging over realizations of the Poisson process.

Now take a set of cells indexed by i where the mean number m_i fluctuates in space

$$m_i = \int d^3x W_i(\mathbf{x}) n(\mathbf{x}; z_i), \quad (2)$$

where $W_i(\mathbf{x})$ is the cell window function, in this case a top hat, and $n(\mathbf{x}; z_i)$ is the spatial number density. On

large scales, fluctuations in their spatial number density trace the linear density fluctuations $\delta(\mathbf{x}; z)$ from the large scale structure of the universe

$$n(\mathbf{x}; z) = \bar{n}(z)[1 + b(z)\delta(\mathbf{x}; z)], \quad (3)$$

where b is the linear bias of the clusters. Overbars denote a spatial average or a sample average over realizations of the large scale structure. Thus the sample averaged number counts $\bar{m}_i = V_i \bar{n}(z_i)$ where the cell volume is $V_i \equiv \int d^3x W_i$.

The mean numbers then possess a sample covariance given by the linear power spectrum $P(k)$ [9]

$$\begin{aligned} S_{ij} &= \langle (m_i - \bar{m}_i)(m_j - \bar{m}_j) \rangle_S \\ &= \frac{b_i \bar{m}_i b_j \bar{m}_j}{V_i V_j} \int \frac{d^3k}{(2\pi)^3} W_i^*(\mathbf{k}) W_j(\mathbf{k}) P(k). \end{aligned} \quad (4)$$

Here $W_i(\mathbf{k})$ is the Fourier transform of $W_i(\mathbf{x})$ and $b_i = b(z_i)$. For a single spherical cell of comoving radius R , the fractional errors $S_{ii}^{1/2}/m_i = b_i \sigma_R$ where σ_R is the rms linear density fluctuation in the cell.

The likelihood of drawing a set of cluster counts $\mathbf{N} = (N_1, \dots, N_c)$ given a model for $\bar{\mathbf{m}}$ and \mathbf{S} is then

$$L(\mathbf{N}|\bar{\mathbf{m}}, \mathbf{S}) = \int d^c m \left[\prod_{i=1}^c P(N_i|m_i) \right] G(\mathbf{m}|\bar{\mathbf{m}}, \mathbf{S}), \quad (5)$$

where G denotes the multivariate Gaussian distribution

$$G(\mathbf{m}|\bar{\mathbf{m}}, \mathbf{S}) = \frac{1}{\sqrt{(2\pi)^c \det \mathbf{S}}} e^{-\frac{1}{2}(\mathbf{m}-\bar{\mathbf{m}})\mathbf{S}^{-1}(\mathbf{m}-\bar{\mathbf{m}})}. \quad (6)$$

It is instructive to consider a few special cases. In the limit that sample variance is negligible compared with the Poisson variance $S_{ii} \ll \bar{m}_i$ the Gaussian approximates a delta function and

$$L(\mathbf{N}|\bar{\mathbf{m}}, \mathbf{S}) \approx \prod_{i=1}^c P(N_i|\bar{m}_i). \quad (7)$$

This form is appropriate for very rare clusters and is used in the analysis of local high temperature clusters.

In the limit of large numbers $m_i \gg 1$, the Poisson distribution approaches a Gaussian

$$\prod_{i=1}^c P(N_i|\bar{m}_i) \approx G(\mathbf{N}|\mathbf{m}, \mathbf{M}), \quad (8)$$

where $\mathbf{M} = \text{diag}(\mathbf{m}_i)$. The likelihood becomes a convolution of Gaussians

$$L(\mathbf{N}|\bar{\mathbf{m}}, \mathbf{S}) \approx \int d^c m G(\mathbf{N}|\mathbf{m}, \mathbf{M}) G(\mathbf{m}|\bar{\mathbf{m}}, \mathbf{S}), \quad (9)$$

or via the convolution theorem approximately a Gaussian in $\mathbf{N} - \bar{\mathbf{m}}$ with covariance $\mathbf{C} \equiv \mathbf{S} + \bar{\mathbf{M}}$.

The statistical properties of the counts are hence specified by their mean $\bar{\mathbf{m}}$ and their sample covariance \mathbf{S} . The space density $\bar{n}(z)$ controls $\bar{\mathbf{m}}$ and hence the ‘‘signal’’; the bias $b(z)$ controls \mathbf{S} and hence the ‘‘noise’’. Given a cosmology, both \bar{n} and b can be predicted as a function of the cluster mass (see §IV). From the perspective of mass calibration both ingredients are therefore signal.

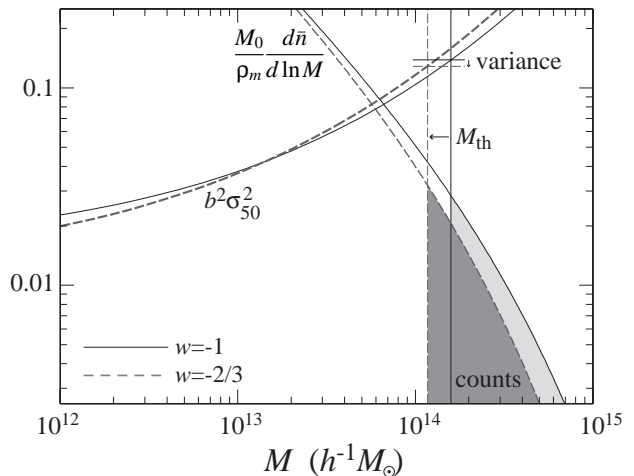


FIG. 1: Mass sensitivity of the counts and their variance compared with sensitivity to the dark energy equation of state w at $z = 0$. The integral of the mass function $d\bar{n}/d\ln M$, here normalized to $M_0 = 10^{14} h^{-1} M_\odot$ from the threshold M_{th} predicts the expected counts. Changes due to w can be compensated by a comparable shift in M_{th} (dark vs. light shaded region) but also change the fractional cell variance at threshold (horizontal lines), shown here normalized to the typical cell volume ($50 h^{-1}$ Mpc radius) as $b^2 \sigma_{50}^2$.

III. FISHER MATRIX

The Fisher matrix formalism provides a means of making projections for the result of likelihood analyses of future data given a parameterized model for the mean $\bar{\mathbf{m}}$ and sample covariance \mathbf{S} of the counts as well as a fiducial choice of the true parameters.

Given a set of parameters p_α on which these quantities depend, the information is quantified by the Fisher matrix

$$F_{\alpha\beta} \equiv -\left\langle \frac{\partial^2 \ln L}{\partial p_\alpha \partial p_\beta} \right\rangle \quad (10)$$

such that the parameter covariance matrix $C_{\alpha\beta} \approx (\mathbf{F}^{-1})_{\alpha\beta}$. The marginalized parameter errors are then $\sigma(p_\alpha) = C_{\alpha\alpha}^{1/2}$.

Again let us begin by considering the limiting cases. In the case of negligible sample covariance

$$F_{\alpha\beta} = \sum_i \frac{1}{\bar{m}_i} \bar{m}_{i,\alpha} \bar{m}_{i,\beta} = \bar{\mathbf{m}}_{,\alpha}^t \bar{\mathbf{M}}^{-1} \bar{\mathbf{m}}_{,\beta}, \quad (11)$$

where $, \equiv \partial/\partial p_\alpha$ [10]. In the case of negligible Poisson errors [11]

$$F_{\alpha\beta} = \bar{\mathbf{m}}_{,\alpha}^t \mathbf{S}^{-1} \bar{\mathbf{m}}_{,\beta} + \frac{1}{2} \text{Tr}[\mathbf{S}^{-1} \mathbf{S}_{,\alpha} \mathbf{S}^{-1} \mathbf{S}_{,\beta}]. \quad (12)$$

Notice that even in the $m_i \gg 1$ Gaussian limit, the Poisson Fisher matrix does not carry a term involving the derivatives of the variance $\mathbf{M}_{,\alpha}$. However the fractional error induced by including such a term scales as m_i^{-1} and is therefore negligible in this limit.

Given these two limits, we approximate the full Fisher matrix as

$$F_{\alpha\beta} = \bar{\mathbf{m}}_{,\alpha}^t \mathbf{C}^{-1} \bar{\mathbf{m}}_{,\beta} + \frac{1}{2} \text{Tr}[\mathbf{C}^{-1} \mathbf{S}_{,\alpha} \mathbf{C}^{-1} \mathbf{S}_{,\beta}], \quad (13)$$

where recall $\mathbf{C} = \mathbf{S} + \bar{\mathbf{M}}$. The two pieces represent the contribution to the information on the parameters from the mean of the cell counts and their cell-to-cell (co)variance induced by structure in the universe.

IV. SELF-CALIBRATION

The two sources of information, the mean counts and their cell-to-cell variance, depend differently on the cluster mass. By comparing the two one can in principle solve for the mass and hence remove the calibration uncertainty in the interpretation of the number counts.

Given an initial power spectrum, simulations can reliably predict the number density of dark matter halos associated with clusters of a given mass. For illustrative purposes, we will employ the fitting function [12]

$$\frac{d\bar{n}}{d \ln M} = 0.3 \frac{\rho_m}{M} \frac{d \ln \sigma^{-1}}{d \ln M} \exp[-|\ln \sigma^{-1} + 0.64|^{3.82}], \quad (14)$$

where $\sigma^2(M; z) \equiv \sigma_R^2(z)$, the density field variance in a region enclosing $M = 4\pi R^3 \rho_m / 3$ at the mean matter density today ρ_m . Likewise the bias of these objects can be described by [13, 14]

$$b(M; z) = 1 + \frac{a\delta_c^2/\sigma^2 - 1}{\delta_c} + \frac{2p}{\delta_c[1 + (a\delta_c^2/\sigma^2)^p]} \quad (15)$$

with $a = 0.75$, $p = 0.3$, and $\delta_c = 1.69$. Though these relations must be replaced by numerical results in a real analysis, self-calibration will still be possible so long as the bias and mean number counts scale with the mass of the objects in a predictable way.

Consider now a selection that is defined by a threshold in some observable quantity such flux or temperature. Let us define the relationship between the observable threshold f_{th} and the mass threshold by two parameters A and m [8]

$$\frac{M_{\text{th}}}{M_0(z)} = e^A (1+z)^m \left(\frac{f_{\text{th}}}{f_0} \right)^p, \quad (16)$$

where f_0 is an arbitrary normalization parameter, $M_0(z)$ characterizes an a priori guess for the relation such that deviations can be described by a power law in $(1+z)$, and p is considered known (see [7] for a generalization to arbitrary $p(z)$). Then the statistical model of the counts is defined through Eqn. (3) and (4)

$$\begin{aligned} \bar{n}(z) &= \int_{\ln M_{\text{th}}(z)}^{\infty} d \ln M \frac{d\bar{n}}{d \ln M}, \\ b(z) &= \frac{1}{\bar{n}} \int_{\ln M_{\text{th}}(z)}^{\infty} d \ln M \frac{d\bar{n}}{d \ln M} b(M; z). \end{aligned} \quad (17)$$

In reality the mass-observable relation will contain finite scatter which will blur the threshold; this scatter must also be modeled in a real analysis. We use this simple prescription for illustrative purposes only.

Fig. 1 illustrates the self-calibration idea. If only the counts are considered, changes in the cosmology are degenerate with those in the threshold. However lowering the threshold to compensate a smaller amplitude of density fluctuations has two effects on the variance of counts that break the degeneracy: it lowers the variance due to the decreased underlying linear structure but also makes objects at a fixed mass rarer and hence more highly biased.

We approximate the results of a joint likelihood analysis of the mass-observable and cosmological parameters via the Fisher matrix. We take the cosmological parameters as the normalization of the initial curvature spectrum $\delta_\zeta (= 5.07 \times 10^{-5})$ at $k = 0.05 \text{ Mpc}^{-1}$ (see [15] for its relationship to the more traditional σ_8 normalization), its tilt $n (= 1)$, the baryon density $\Omega_b h^2 (= 0.024)$, the dark matter density $\Omega_m h^2 (= 0.14)$, and the 2 dark energy parameters of interest: its density $\Omega_{\text{DE}} (= 0.73)$ and equation of state $w (= -1)$ which we assume to be constant. Values in the fiducial cosmology are given in parentheses. The first 4 parameters have already been determined at the few to 10% level through the CMB [16] and we will extrapolate these constraints into the future with priors of $\sigma(\ln \delta_\zeta) = \sigma(n) = \sigma(\ln \Omega_b h^2) = \sigma(\ln \Omega_m h^2) = 0.01$.

For illustrative purposes let us take a fiducial cluster survey with specifications similar to the planned South Pole Telescope (SPT) Survey: an area of 4000 deg² and a sensitivity corresponding to a constant $M_0 = M_{\text{th}}|_{\text{fid}} = 10^{14.2} h^{-1} M_\odot$. We divide the number counts into bins of redshift $\Delta z = 0.1$ and 400 angular cells of 10 deg² and vary the maximum redshift z_{max} for which photometric redshifts will be available. With these large cell sizes, the covariance between neighboring cells is negligible, considerably simplifying the analysis.

Constraints in the $\Omega_{\text{DE}} - w$ dark energy plane from counts alone are severely compromised by mass threshold uncertainties (see Fig. 2). This is especially true for the lower z_{max} since the lever arm is not sufficient to distinguish between the power law deviations in the mass-observable relation and the dark energy. Here the errors in Ω_{DE} degrade by factor of 37 and w by a factor of 4.6. Much of the dark energy information is restored by including variance information. For $z_{\text{max}} = 1$, errors improve by a factor of 7.5 to $\sigma(\Omega_{\text{DE}}) = 0.04$ and a factor of 2 to $\sigma(w) = 0.09$.

Self-calibration also makes the errors more robust to z_{max} , for $z_{\text{max}} = 2$, $\sigma(\Omega_{\text{DE}}) = 0.03$ and $\sigma(w) = 0.06$. These results are also relatively insensitive to the cell size. For 4 deg² cells or $\Delta z = 0.05$ the errors remain nearly the same. Likewise, the relative improvement due to self-calibration is relatively insensitive to the mass threshold assumed. Finally errors on the actual calibration parameters are $\sigma(A) = \sigma(m) = 0.14$ for $z_{\text{max}} = 2$.

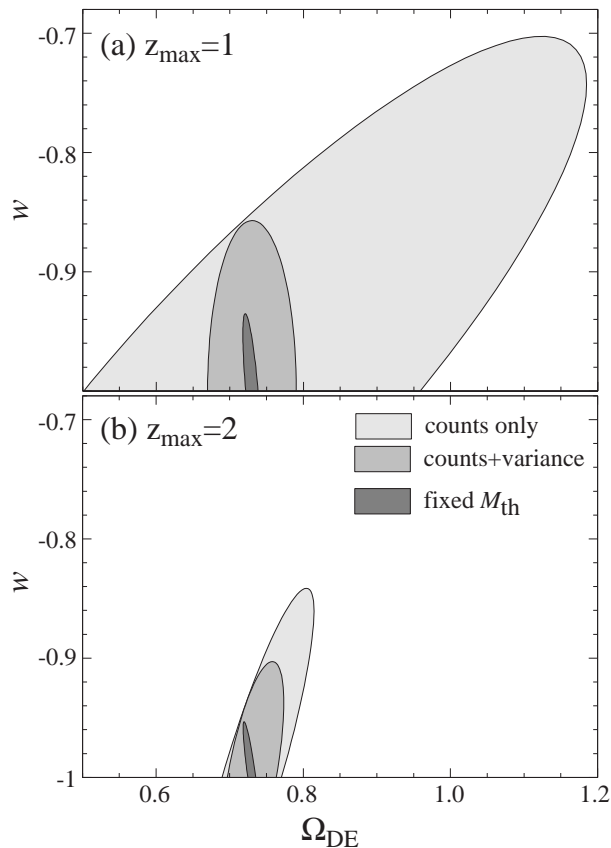


FIG. 2: Projected constraints in the $\Omega_{\text{DE}} - w$ dark energy plane (68% CL) for the fiducial survey and a maximum redshift of (a) $z_{\text{max}} = 1$ and (b) $z_{\text{max}} = 2$. Unknown power law evolution in the mass-observable relation degrades constraints from the inner most to outermost ellipses if only the abundance or counts is used. By adding in information from the count variance, the survey partially self-calibrates leading to the middle ellipses.

V. DISCUSSION

Cluster number count surveys contain information not only in the mean counts but also in their cell-to-cell variance. The latter depends on the clustering of clusters and hence provides an independent constraint on their mass. This information automatically comes out of a full likelihood analysis of the counts and provides an opportunity for self-calibration of the survey.

In the idealized case where the scatter in the mass-observable relation is low and known, self-calibration via the variance improves dark energy constraints for power law evolution in the mass threshold by a factor of 2-10 depending mainly on the maximum redshift for which accurate photometric redshifts can be obtained. In principle, self-calibration can constrain a more arbitrary evolution, e.g. an independent mass-observable relation for each redshift slice. In practice, the resulting dark energy constraints are then too weak to be of interest ($\sigma(\Omega_{\text{DE}}) = 0.07$, $\sigma(w) = 0.57$ in the fiducial survey). Likewise, for an unknown scatter in the mass-observable relation, variance self-calibration alone is unlikely to suffice. In these cases it can be supplemented with selections at various thresholds in the observable [7] or with the full angular power spectra of the cell counts (e.g. [15]) though a full treatment is beyond the scope of this work.

Since self-calibration involves only information which exists in the survey itself, it comes at no additional observational cost. It therefore complements potentially more precise but costly cross-calibration studies.

Acknowledgments: We thank A. Kravtsov and J. Mohr for useful discussions. This work was supported by NASA NAG5-10840, the DOE, the Packard Foundation and CNPq; it was carried out at the CfCP under NSF PHY-0114422.

-
- [1] V.R. Eke, S. Cole and C.S. Frenk, *Mon. Not. R. Astron. Soc.*, **282**, 263 (1996); J.P. Henry, *Astrophys. J.*, **489**, 1 (1997); N.A. Bahcall and X. Fan, *Astrophys. J.*, **504**, 1 (1998); A. Blanchard and J.G. Bartlett, *Astron. Astrophys.*, **332**, L49 (1998); P.T.P. Viana and A.R. Liddle, *Mon. Not. R. Astron. Soc.*, **303**, 535 (1999).
 - [2] L. Wang and P.J. Steinhardt, *Astrophys. J.*, **508**, 483 (1998).
 - [3] Z. Haiman, J.J. Mohr and G.P. Holder, *Astrophys. J.*, **553**, 545 (2001).
 - [4] E. Pierpaoli, D. Scott and M. White, *Mon. Not. R. Astron. Soc.*, **325**, 77 (2001).
 - [5] U. Seljak, *Mon. Not. R. Astron. Soc.*, **337**, 769 (2002).
 - [6] E.S. Levine, A.E. Schulz and M. White, *Astrophys. J.*, **577**, 569 (2002).
 - [7] W. Hu, *Phys. Rev. D*, **67**, 081304 (2003).
 - [8] M. Majumdar and J.J. Mohr, *Astrophys. J.*, submitted, astro-ph/0305341 (2003).
 - [9] W. Hu and A.V. Kravtsov, *Astrophys. J.*, **584**, 702 (2003).
 - [10] G. Holder, Z. Haiman and J.J. Mohr, *Astrophys. J. Lett.*, **560**, 111 (2001).
 - [11] M. Tegmark, A.N. Taylor and A.F. Heavens, *Astrophys. J.*, **480**, 22 (1997).
 - [12] A. Jenkins, *et al.* *MNRAS*, **321**, 372 (2001).
 - [13] H.J. Mo and S.D.M. White, *Mon. Not. R. Astron. Soc.*, **282**, 347 (1996).
 - [14] R.K. Sheth and B. Tormen, *Mon. Not. R. Astron. Soc.*, **308**, 119 (1999).
 - [15] W. Hu and B. Jain, *Phys. Rev. D*, submitted, astro-ph/0312395 (2003).
 - [16] D.N. Spergel, *et al.* *Astrophys. J. Supp.*, **148**, 175 (2003).